Synthesis, Structure and Properties of Crystalline and Nanocrystalline $MnPS_3$-Poly(Phenylene Vinylene) Intercalates

Ivonne M. Diaz Mesa, Peter J. S. Foot* and Roman A. Kresinski

Materials Research Centre, Faculty of SEC, Kingston University London

Penrhyn Road, Kingston upon Thames KT1 2EE (U.K.)

* Corresponding Author. Email: p.j.foot@kingston.ac.uk

Tel.: (+44)20 84172485

Abstract

The preparation of luminescent semiconducting nanocomposites of crystalline and amorphous manganese phosphorus trisulfide ($MnPS_3$), containing intercalated poly(phenylene vinylene) [PPV] is reported. The materials were characterized by thermogravimetric analysis, infrared and Raman spectroscopy and X-ray diffractometry. Scanning electron microscopy was used to monitor the crystallinity and morphology of the host materials.

An average increase of 5.05 Å in the interlayer distance of $MnPS_3$ was observed by XRD, as a result of the intercalation of PPV. The resulting composite materials presented more stable photoluminescent properties than unintercalated PPV, and with slightly blue-shifted emission; they exhibited significantly higher electronic conductivities than $MnPS_3$ or the polymer alone. The effects of the intercalation host on the optical and electronic properties of the PPV guest are discussed.

KEYWORDS: A. Chalcogenides; A. Layered Compounds; A. Organic Compounds; B. Intercalation Reactions; B. Luminescence.

Highlights:

- First report of poly(phenylene vinylene) intercalation in layered $MnPS_3$
- Compares systems based on high- and low-temperature synthesized $MnPS_3$
- Structural and spectroscopic studies of the intercalates
- The hybrid organic-inorganic materials show stable photoluminescence
- Electronic conductivity is increased after the intercalation reaction

1. Introduction

Poly(p-phenylene vinylene) (PPV) is one of the most-studied electroluminescent conjugated polymers. It exhibits bright yellow-green fluorescence with an emission maximum at 551 nm (2.25 eV), and that property made it a prototype polymer for light-emitting diodes. Its electrical conductivity is enhanced upon oxidation (or reduction), which creates mobile radical ions and makes it a p-type (or n-type) semiconductor. However, like all opto-electronic polymers, it can degrade in the presence of oxygen and moisture; this results in the formation of crosslinks between the polymer chains, loss of delocalization and decreased electronic conductivity [1-3].

A possible solution to such problems is to synthesize composites containing the emissive polymer inside a lamellar-structured inorganic host that can accommodate organic molecules between its layers. The geometrical restrictions imposed by the inorganic host could result in better-organized polymer chains that would facilitate charge injection and transfer between the conducting units. Several research groups have reported the formation of composites of PPV and inorganic two-dimensional insulators [4-7]; however, intercalates of PPV between the layers of transparent semiconducting divalent metal thiohypophosphates ($M^{II}PS_3$ or $M^{II}_2P_2S_6$) and their luminescent properties have not been explored. In this paper, we report the synthesis and characterization of luminescent organic-inorganic composites containing PPV-intercalated $MnPS_3$.

The divalent metal thiohypophosphates are layer-structured compounds that have been studied by several research groups, mostly due to their ability to intercalate guest molecules, forming organic-inorganic materials with interesting magnetic and electronic properties [8-11]. In addition to their versatile intercalation chemistry, $M^{II}PS_3$ materials are often quite transparent in the visible region, which makes them ideal hosts for luminescent polymers with optoelectronic applications [12].

MPS_3 compounds are usually prepared as macroscopic crystals by high-temperature techniques [8-11]; however, they can also be produced as colloidal nanoparticles in aqueous solution at room temperature. This was first done by Foot *et al* [13] by mixing a source of thiohypophosphate $(P_2S_6)^{4-}$ anions and a solution of M^{2+} cations. The process results in the production of large quantities of amorphous or

nanocrystalline MPS_3 with analogous properties to those made by the inconvenient solid-state synthesis at high temperatures. Moreover, the crystallinity can be readily increased by annealing the products at about 300^{o}C for 2 to 4 h [13]. This method permits the production of thin-film coatings suitable for photovoltaic or photo-electrochemical applications.

One of the sources of $(P_2S_6)^{4-}$ used in the low-temperature route was the soluble sodium salt $Na_4P_2S_6$, first prepared by Falius [14]. The stoichiometric equation for the synthetic reaction is:

$$\mathbf{6Na_2S + 2PCl_3 + ½O_2 + H_2O \longrightarrow 3Na_4P_2S_6 + 6NaCl + 2NaOH}$$

Colloidal MPS_3 compounds or amorphous precipitates are subsequently formed by reacting solutions of $Na_4P_2S_6$ with solutions of the metal in the M^{2+} state, and the overall reaction can be written as follows:

$$\mathbf{Na_4P_2S_{6\,(aq)} + 2M^{2+}_{(aq)} \longrightarrow 2MPS_3 + 4Na^{+}_{(aq)}}$$

The main aim of the present work was to synthesize and study manganese (II) thiohypophosphate ($MnPS_3$ or $Mn_2P_2S_6$) as a host material for the preparation of conjugated polymer/inorganic composites. Much previous investigation has been carried out on other MPS_3 intercalates of simple molecules, but this work has focused on the intercalation of the luminescent semiconductor PPV into $MnPS_3$.

As well as synthesizing single crystals and polycrystalline samples of $MnPS_3$ by the conventional high temperature method, we have used the alternative low-temperature route to produce them from colloidal suspensions, and have studied the physical and spectroscopic properties of the resulting nanocomposite materials with PPV.

2. Experimental

The overall synthetic strategy is outlined in Scheme 1.

Scheme 1

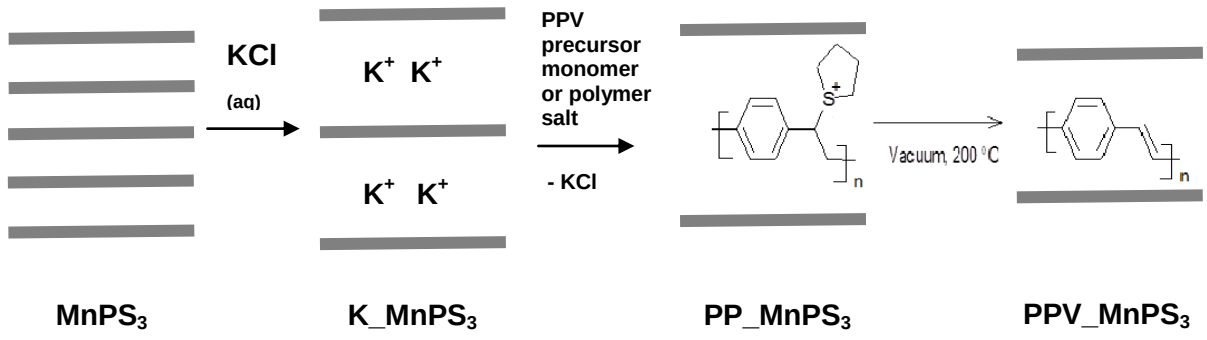

$MnPS_3$ **K_$MnPS_3$** **PP_$MnPS_3$** **PPV_$MnPS_3$**

Abbreviations:

$MnPS_3$: $MnPS_3$ synthesized by a solid-state reaction at high temperature.

$MnPS_3$_LT: $MnPS_3$ synthesized by solution chemistry at room temperature.

K_$MnPS_3$: K^+-intercalated $MnPS_3$

PP_$MnPS_3$: PPV precursor polymer-intercalated $MnPS_3$

PPV_$MnPS_3$: PPV-intercalated $MnPS_3$

PPV_$MnPS_3$_LT: PPV-intercalated $MnPS_3$_LT

2.1 Synthesis of intercalated composites

Intercalation of $MnPS_3$ (obtained by high-temperature synthesis)

All chemicals were purchased from Sigma Aldrich Ltd., UK, and used without further purification.

2.1.1 Synthesis of p-xylylene-bis(tetrahydrothiophenium chloride) (monomer) and poly(p-xylylene-bis(tetrahydrothiophenium chloride) *(PPV precursor polymer*)

Both of the above salts were synthesized by following the route described by Wessling and Zimmerman [15].

2.1.2 Synthesis of $MnPS_3$

Stoichiometric amounts of sulfur (99.9 %) (2.12 g; 0.06 mol), red phosphorus (99.9%) (1.02 g; 0.03 mol) and manganese (II) sulfide (99.9%) (1.81 g, 0.02 mol)

were sealed in 20 cm long evacuated quartz tubes. The tubes were then heated at 720^{o}C with a linear temperature gradient to form crystalline products by sublimation at 680^{o}C, in a 3-zone tube furnace for 4 weeks, according to established methods [8,11].

Green polycrystalline material and thin platelet crystals were obtained from the crystal growth ampoule. The single crystals were typically about 1.4 x 1.2 x 0.03 mm^3. ICP analysis of a sample (single crystal) after dissolution in aqua regia led to the approximate formula $Mn_{0.93}P_{1.0}S_{3.3}$, but powder x-ray diffractometry (see below) only gave peaks in accordance with those for the stoichiometric compound, $Mn_2P_2S_6$ (JCPDS file #33-0903). Yield obtained: 4.38 g (73 %).

2.1.3 Potassium ion intercalation*:* Single crystals of $MnPS_3$ (0.04 g; 2.14 x10^{-4} mol) were added to an aqueous solution of KCl (5.0 mL; 2M). The mixture was stirred for 2 h at ambient temperature. The solid was filtered off, washed with distilled water and dried under vacuum for 24 h at 80 ^{0}C. The product obtained (designated K_$MnPS_3$) was $K_{0.5}Mn_{0.75}PS_3$. Yield: 0.020 g (44 %).

2.1.4 PPV intercalation: K_$MnPS_3$ crystals (0.06 g; 2.73 x10^{-4} mol) were added to a methanolic solution of the precursor monomer p-*xylylene-bis(tetrahydrothiophenium chloride)* (11 mL; 0.2 M). The mixture was left stirring for 24 h under nitrogen; then it was cooled to 0 ^{o}C and NaOH (11 mL; 0.2 M; 0 ^{o}C) was added, after which it was stirred for a further hour. HCl (1M) was then added to neutralize it, and stirring was continued for two more hours, keeping the mixture at 0^{o}C throughout the reaction. A green-yellow suspension was formed, containing the intercalated crystals, and it was dialyzed against water (3 x 2 L) for 3 days to remove K^+, Mn^{2+}, Na^+ and Cl^- ions. After this, the intercalated crystals containing poly(p-xylylene-bis(tetrahydrothiophenium chloride) (PPV precursor polymer) were filtered off, washed with methanol several times and then dried. Finally, they were placed under a stream of nitrogen and heated to 230^{o}C for 30 min to convert the precursor to PPV.

2.2 Intercalation of $MnPS_3$ (obtained by ambient-temperature solution route)

$Na_4P_2S_6.6H_2O$ was synthesized according to the literature method of Falius [14].

Two micellar solutions were prepared separately, using a similar approach to one in the literature [16,17]. One of them contained Brij-97 surfactant (3.2 g) in cyclohexane

(40 mL), aqueous $MnCl_2.4H_2O$ (0.02 g in 1.5 mL H_2O) and precursor polymer solution (5 mL, 0.2 M). The other solution contained Brij-97 (4.0 g) in cyclohexane (50 mL) and $Na_4P_2S_6.6H_2O$ (0.03 g in 3 mL H_2O). The two solutions were mixed and left stirring for 48 h, and ethanol (30 mL) was then added to break the emulsion; the precipitate formed was collected, washed several times with ethanol and dried in air for 24 h. The samples were heated under nitrogen for 1 h at 220 ^oC to convert the precursor to PPV.

2.3 Characterization

X-ray powder diffractometry (XRD) was carried out on a Bruker-AXS D8 Advance instrument, with Cu Kα radiation (λ = 1.542 Å). All samples were finely powdered and were spread onto double-sided adhesive tape (Sellotape) to form thin films for XRD analysis. SEM images were obtained using a Zeiss EVO 50 with an Oxford Instruments INCA analytical suite. Attenuated total reflection infrared (ATR-IR) spectroscopy was carried out using a Thermo Scientific Nicolet IS5 iD5 ATR, with 16 scans, over the range 650-4000 cm^{-1}. Raman spectroscopy was performed on a Renishaw inVia Raman Microscope, with WiRE 3.3 software and Renishaw MS20 encoded mechanical stage. A He-Ne 633nm, 500mW laser (typically 8mW emission) was used.

Photoluminescence studies using a Varian Cary Eclipse Spectrofluorimeter were carried out on single crystals mounted onto black substrates and on polymer films coated onto quartz slides. In both cases, the substrates were positioned at an angle of about 60^o to the incident beam, to avoid the effects of direct specular reflection from the quartz slides.

Electrical conductivity measurements were carried out on single crystals of $MnPS_3$ and of PPV-intercalated $MnPS_3$. Sample holders were designed to fix the small crystals in position, and the conductivity was measured on the basal planes (parallel to the layers) using four-in-line gold electrodes. In the case of the polycrystalline and amorphous materials, the samples were powdered and pressed into disks (5 mm diameter). The disks were placed in a PTFE cell to make guarded two-probe measurements using spring-loaded silver-coated copper electrodes. Sample thicknesses were determined by means of a digital micrometer. A Keithley 195

current source and a Keithley 197 electrometer were used to make the electrical measurements under computer control.

3. Results and Discussion

3.1 High-Temperature (Crystalline) $MnPS_3$

3.1.1 Scanning Electron Microscopy (SEM)

The morphology of the samples was studied by SEM. Clear lamellar structures were observed for the pristine crystalline $MnPS_3$, indicating the regular stacking of the compound (Figure 1 a), but the morphology of the crystals was slightly affected by the intercalation process. After inclusion of the K^+ ions and subsequently the polymer, the samples retained their lamellar structure, although more defects such as cracks and ragged edges were observed (Figure 1 b), due to the mechanical stress that the crystals underwent during the insertion of guest molecules.

a. 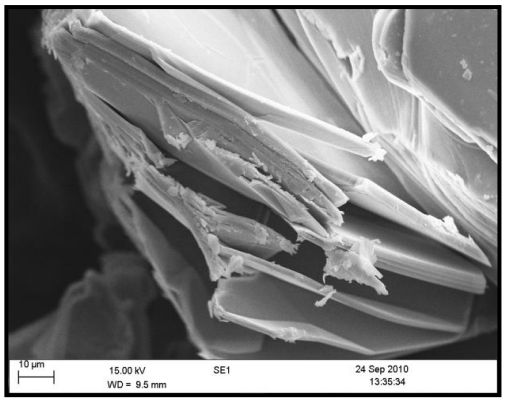

b. 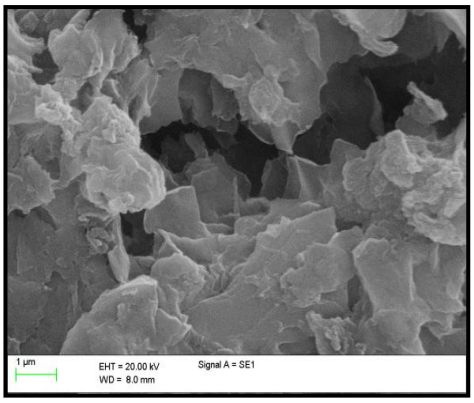

Figure 1: SEM images of a. crystalline $MnPS_3$ and b. PPV_$MnPS_3$. After intercalation of the polymer, the lamellar structure of $MnPS_3$ was preserved.

3.1.2 X-Ray Diffraction (XRD)

The structure of $MnPS_3$ was confirmed through the XRD pattern shown in Figure 2(a). The first (001) reflection was observed at 13.58^o (2θ) corresponding to the interlayer space (d) of 6.52 Å, followed by an 002 reflection at 27.52^o, equivalent to 3.24 Å. Other peaks present were all typical of the $MnPS_3$ monoclinic space group, in agreement with values in the literature [8-10].

After K^+ intercalation, the product retained its lamellar structure and good crystallinity, as evidenced by the sharp, clear peaks observed in the XRD pattern [Figure 2(b)]. A new (0 0 *ℓ*) peak was observed at 9.84° (2θ) indicating an interlayer spacing of 8.99 Å; i.e. an expansion of 2.47 Å. The crystallographic changes were consistent with literature data for $MnPS_3$ intercalated by K^+ ions [8,18].

The achievement of organic cation exchange intercalation was confirmed by the x-ray patterns shown in Figure 2(c). The diffraction peaks of neither K_$MnPS_3$ nor pristine $MnPS_3$ were observed; instead, new (*0 0 ℓ*) peaks corresponding to an interlayer spacing of 11.58 Å were detected. The 5.13 Å increase in this spacing was attributed to intercalation of the precursor polymer chains within the van der Waals gap, but with the phenylene rings perpendicular rather than parallel to the host layers [19]. No other peaks were observed. The fact that the K^+ ions were firstly exchanged by the monomer and that the polymer was subsequently formed *in situ* between the layers, permitted the formation of a single-phased product in which the polymer chains could be well organized.

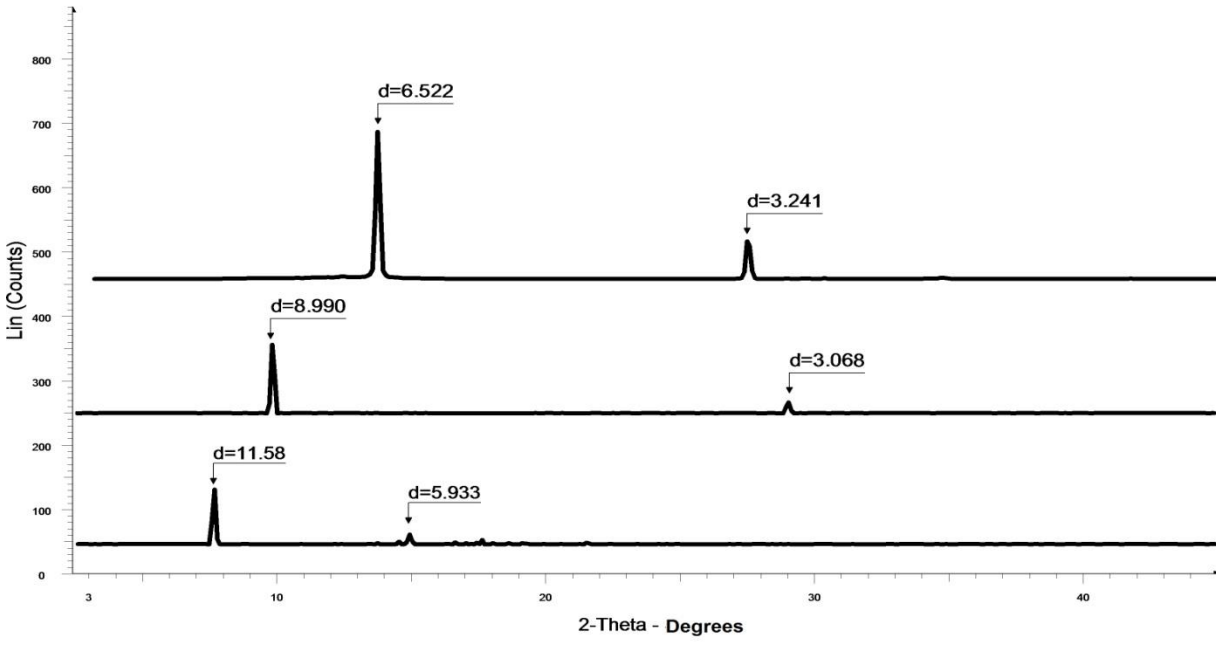

Figure 2: X-ray diffractograms of polycrystalline $MnPS_3$ (top), K^+-intercalated $MnPS_3$ (middle) and PPV_$MnPS_3$ (bottom).

3.1.3 Thermogravimetric Analysis (TGA)

Figure 3 shows the TGA diagram for the precursor polymer-intercalated crystalline $MnPS_3$. The initial (2.0%) decrease in mass, up to about 120^{o}C, was attributed to the loss of water. A significant weight loss (13%) was then observed between 120^o and 380^{o}C; this temperature range is associated with the loss of tetrahydrothiophene (THT) and hydrogen chloride, leading to the formation of the PPV intercalate. On the basis of the TGA data, the approximate proportions of water and of phenylene-vinylene units were respectively 0.22 and 0.20 per $MnPS_3$ formula unit.

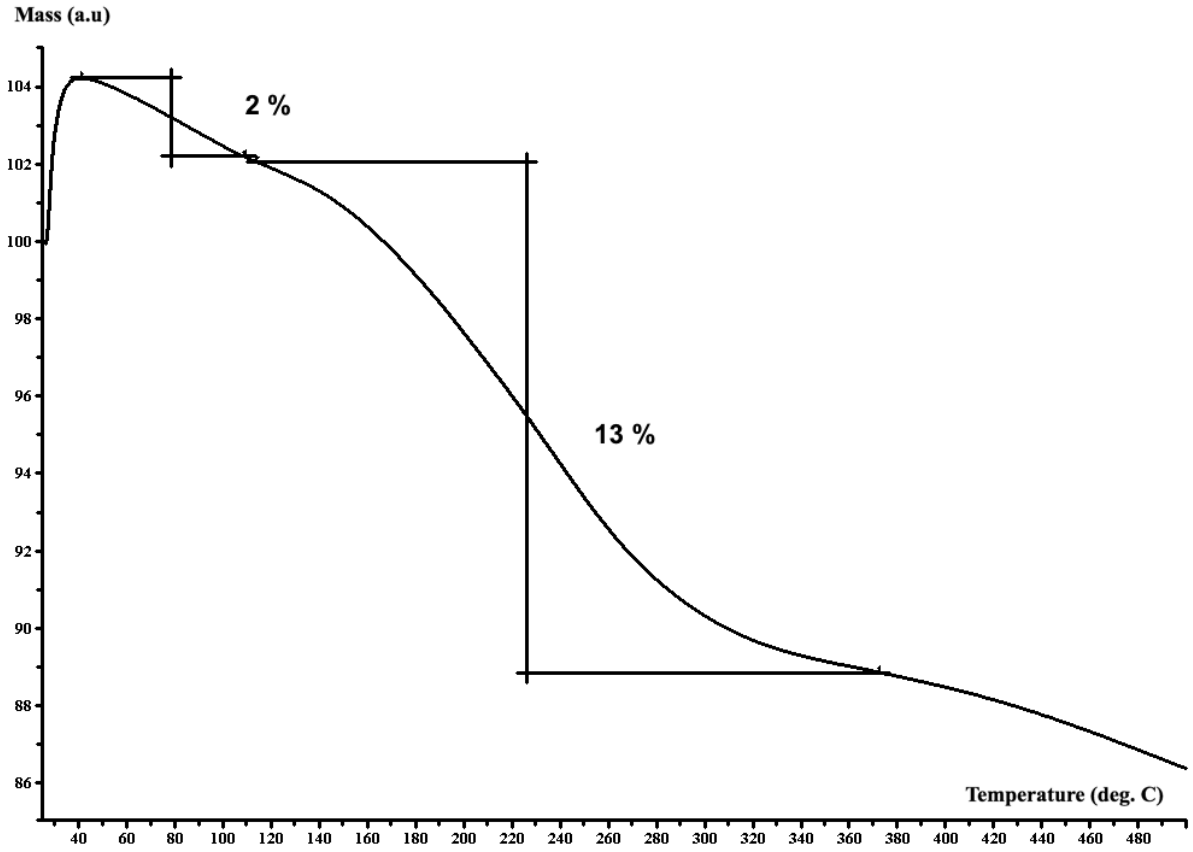

Figure 3: TGA curve of precursor polymer-intercalated $MnPS_3$.

3.1.4 IR and Raman Spectrometry

The main vibrational features of the MPS_3 compounds were found in the region below 600 cm^{-1}. The apparent weak, broad IR band at higher wavenumber in Figure 4 was sample-dependent, and attributable to scattering effects. For pure $MnPS_3$

[Figure 4(a)], the IR spectrum showed the most prominent characteristic vibration of the MPS_3 compounds at 572 cm^{-1}, assigned to the P-S deformation of the P_2S_6 unit of the $M_2P_2S_6$ lattice [19]. The internal modes of $P_2S_6^{4-}$ were represented by the sharp lines at 275 and 383 cm^{-1} in the Raman spectrum. The first one (275 cm^{-1}) was attributed to the S-P-S and S-P-P modes and the second one (383 cm^{-1}) to the mixed symmetric P-P and P-S stretching modes [20]. The low-frequency Raman bands are usually metal-sensitive; hence the weak peak arising at about 154 cm^{-1} was attributed to the M-S bond [20,21] [Figure 4(b)].

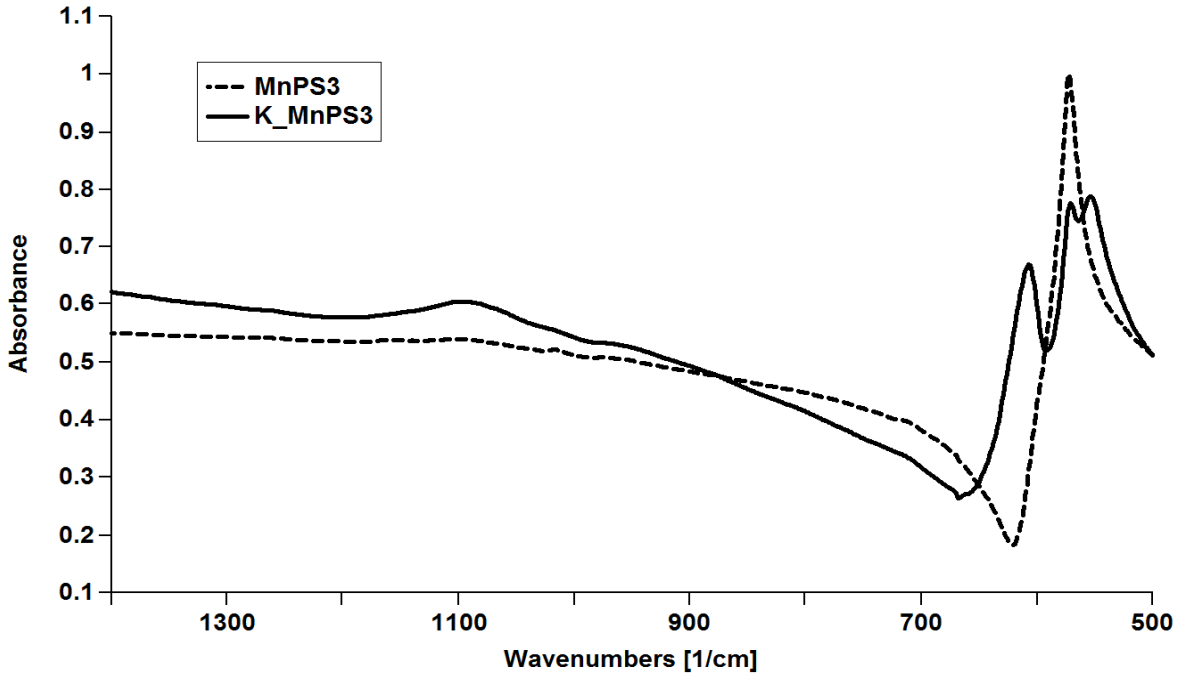

Figure 4a: Infrared absorption spectra of $MnPS_3$ and K^+ intercalated $MnPS_3$.

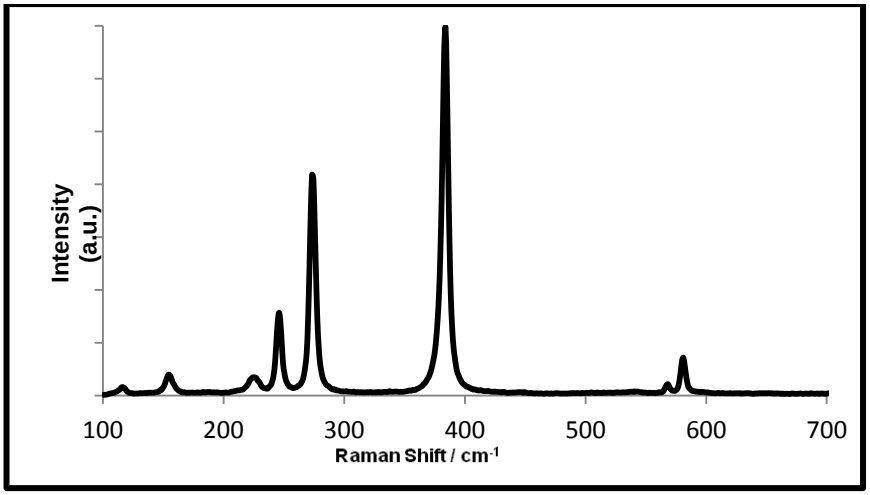

Figure 4b: Raman spectrum of $MnPS_3$

The evidence for intercalation of K^+ was the splitting of the asymmetric deformation band $\nu(PS_3)$ that occurred at 572 cm^{-1} in the IR spectrum of pure $MnPS_3$. The three peaks observed at 553, 572 and 607 cm^{-1} [Figure 4(a)] are characteristic of some intercalated MPS_3 compounds [17]. The normal intercalation mechanism of $MnPS_3$ involves a cation-exchange reaction, wherein M^{2+} ions are released and cation vacancies are formed [17,20]. According to Lagadic *et al* [18], the splitting of the degeneracy of the $\nu(PS_3)$ band is due to the presence of these vacancies, which produce a mixture of P-S bonds, either surrounded by vacancies or still bound to a Mn^{2+} ion.

The IR spectrum of PP_$MnPS_3$ [Figure 5(a)] indicates the presence of the polymer; the spectrum of pure PPV is shown for comparison. The intensity of the organic peaks is fairly low, because the polymer is intercalated inside the inorganic host. The elimination of sulfonium residues and the formation of PPV are indicated by the strong peak at 980 cm^{-1} due to the presence of the *trans* vinylene C-H out-of-plane vibration. A small peak around 3013 cm^{-1} is evident, which corresponds to a *trans* vinylene C-H stretch, characteristic of the conjugated PPV [4,22,23]. Small peaks around 2921 and 2850 cm^{-1} correspond to the sp^3 C-H stretching of the sulfonium leaving-groups of the precursor polymer [4,22,23]. Peaks in the region between 1450 and 1050 cm^{-1} are also characteristic of the sulfonium salt, indicating some persistent traces of the precursor. The split $\nu(PS_3)$ peaks (607 & 553 cm^{-1}) confirm

the presence of the metal vacancies throughout the whole process; no other changes were observed in the IR spectrum of the inorganic host.

The Raman bands at 1551 and 1588 cm^{-1} in Figure 5(b) arise from the ring C-C stretching, and the vinylene C=C stretching vibration is observed at 1632 cm^{-1}; the peak at 1325 cm^{-1} is assigned to the vinylene C=C-H bend, and the strong band around 1170cm^{-1}, commonly found in aromatic compounds, is characteristic of the ring C-H bending vibrations [22, 24-26].

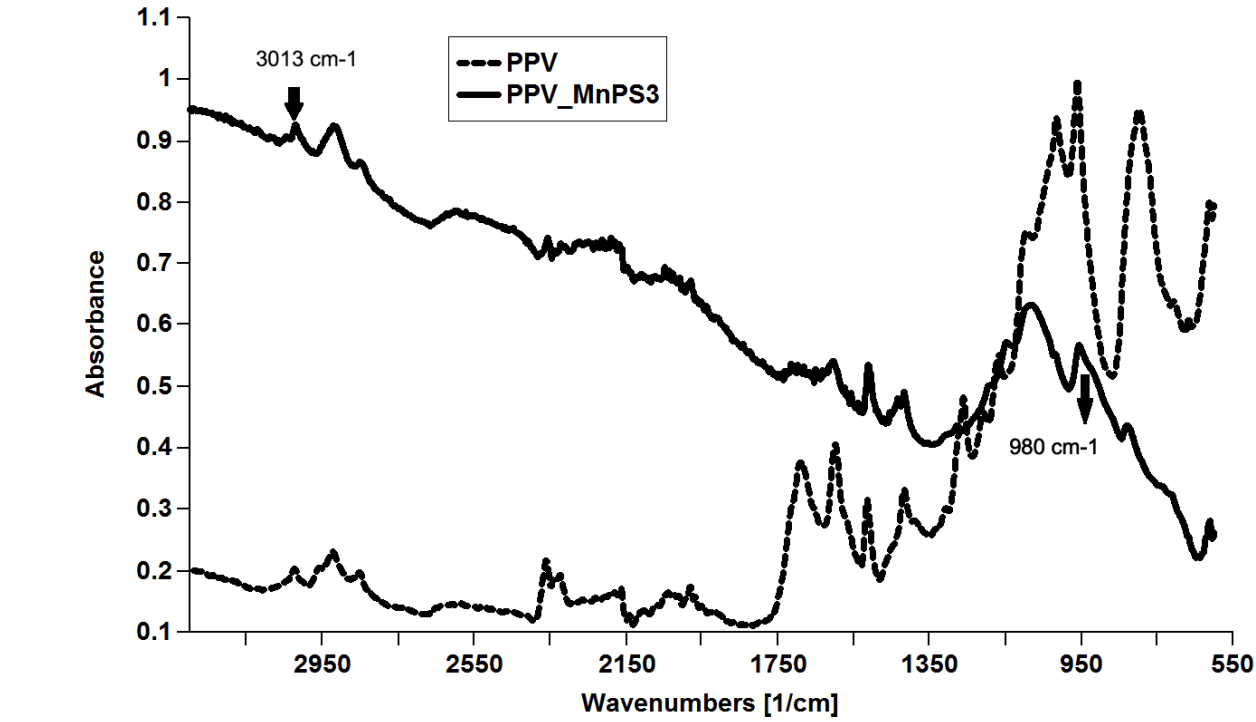

(a)

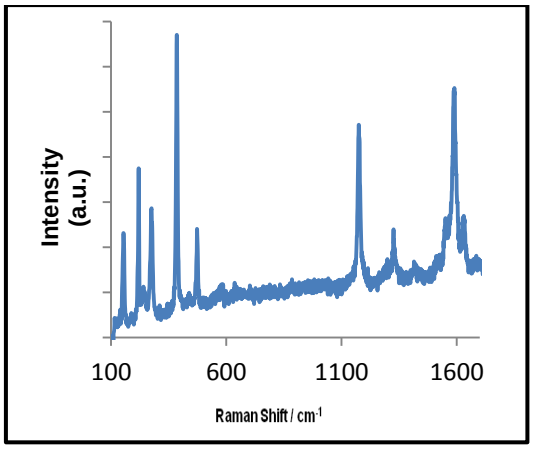

(b)

Figure 5: PPV-intercalated $MnPS_3$ spectra: (a) infrared and (b) Raman.

3.2 Low-Temperature Synthesis of $MnPS_3$ Intercalates

3.2.1 Scanning Electron Microscopy (SEM)

The $MnPS_3$ obtained from solution was initially amorphous, unlike the product of high-temperature synthesis. However, after annealing it in a sealed tube for 30 min at 350^{o}C, the crystallinity was increased (Figure 6), and it was possible to see clear

lamellar features indicating the regular stacking of the compound, like that in the crystalline material.

After the polymer intercalation, the samples retained their lamellar structure (Figure 7).

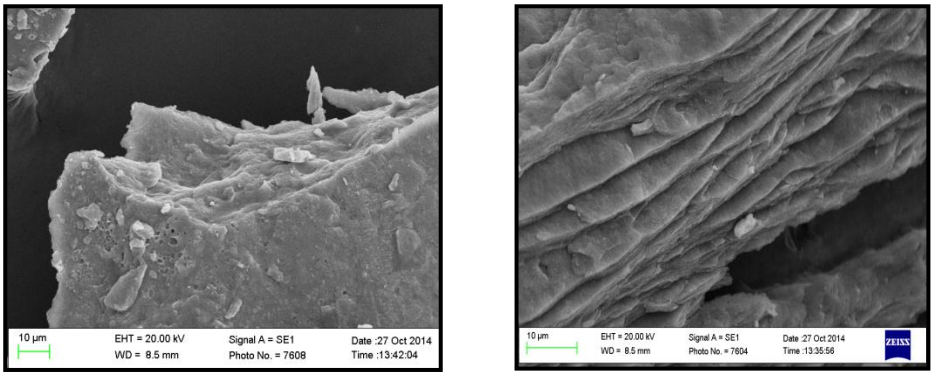

Figure 6: SEM photographs of $MnPS_3$_LT before annealing (left) and after annealing (right).

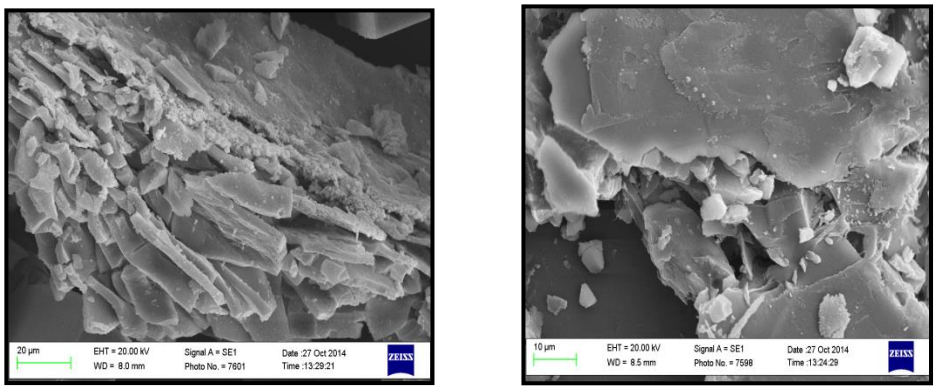

Figure 7: SEM micrographs of PPV-intercalated $MnPS_3$_LT.

3.2.2 X-Ray Diffractometry (XRD)

The samples of $MnPS_3$ obtained by the solution method presented similar structural features to those prepared by direct synthesis; however, the crystallinity of these samples was much lower than that of the high-temperature synthesized phase.

XRD data are listed in the Appendix, Table A1. The main feature was the [0 0 ℓ] reflections, indicating the possible presence of turbostratic disorder; these peaks were used to estimate an interlayer distance of 6.46 Å, a value very similar to that of the high-temperature synthesized $MnPS_3$ [18]. Other peaks at 29.6 and 32.1^o, were

attributed to the 130 and 131 reflections respectively [16]. After annealing the sample, the crystallinity was slightly improved; the peaks became sharper and it was possible to observe the 001, 002 and 003 peaks more clearly (at about 13.9, 28.2 and 41.4^o respectively). The interlayer space was slightly smaller (6.40 Å), possibly due to better atomic organization permitting closer nesting of the $M_2P_2S_6$ lamellae.

The interlayer spacings of $MnPS_3$_LT and its intercalates are given in Table 1. The insertion of the polymer into the van der Waals gap was indicated by a new peak at 6.1^o in the XRD pattern, corresponding to an interlayer expansion of almost 8 Å. This expansion might have been partly due to the insertion of water molecules as well as the polymer; however, the IR spectra did not show any sign of water being present in the final hybrid product. The formation of a double-layer of polymer parallel to the host matrix lamellae seems a more likely reason for such a large interlayer expansion. The other peaks corresponding to pristine amorphous $MnPS_3$ all disappeared after intercalation and formation of PPV, indicating that the registry of the layers had been lost.

Sample	**d_{001} (Å)**	**Interlayer expansion (Å)**
$MnPS_3$_LT	6.46	----------
K_MnPS3_LT	9.21	2.75
PPV_$MnPS_3$_LT	14.23	7.77

Table 1: Interlayer spacing expansion of $MnPS_3$_LT upon intercalation of K^+ and PPV

3.2.3 Thermogravimetric Analysis (TGA)

TGA analysis of $MnPS_3$_LT showed a weight loss of about 5% from 50^o to 150^{o}C. This can be attributed to the elimination of water molecules that were both weakly and strongly bound to the lattice. A subsequent 4.5% weight decrease was attributable to the loss of phosphorus and sulfur from a less-stable amorphous phase, while the more crystalline part only started to decompose above 350^{o}C.

In the case of PPV-intercalated $MnPS_3$_LT, a 10% weight loss was observed between 40^o and 200^{o}C, due to the removal of loosely-bound water molecules. Between 220^o and 340^{o}C, a 35% weight loss step was seen, probably due to the loss of HCl and tetrahydrothiophene from the precursor polymer; it corresponded to the presence of 0.67 monomer units per $MnPS_3$, which is such a large proportion that some of the polymer was apparently present in between the $MnPS_3$ crystallites. The final gravimetric step commenced at around 340^{o}C, and was attributed to the onset of decomposition in the inorganic lattice.

3.2.4 IR and Raman Spectrometry

In the infrared spectrum shown in Figure 8, the strong peak at 2929 cm^{-1} is due to the sp^3 C-H stretching of the sulfonium leaving groups of the precursor polymer, which suggests that only partial conversion had been achieved after heating the samples for 10 min. The bands between 1450 and 1050 cm^{-1} are also characteristic of the sulfonium salts. A small peak at 980 cm^{-1} started to appear, indicating the presence of the *trans*-vinylene C-H out of plane vibration of PPV. Additionally, a weak band around 1100 cm^{-1} was observed, a very sensitive indicator of the formation of phosphates during the intercalation process. The peaks corresponding to the inorganic phase were also present, with the typical $\nu(PS_3)$ band split, which is a signature of intercalated MPS_3 compounds.

The Raman spectra of $MnPS_3$_LT and PPV-intercalated $MnPS_3$_LT are shown in Figure 9. The characteristic PPV vibrations at 1174 and 1630 cm^{-1} are all present in Figure 9(b). The main peaks belonging to the host $MnPS_3$_LT [Figure 9(a)] are all overshadowed by the intense peaks of the conjugated PPV, but it is still possible to see a small peak at 384 cm^{-1} due to the $_{Vsym}(PS_3)$ mode.

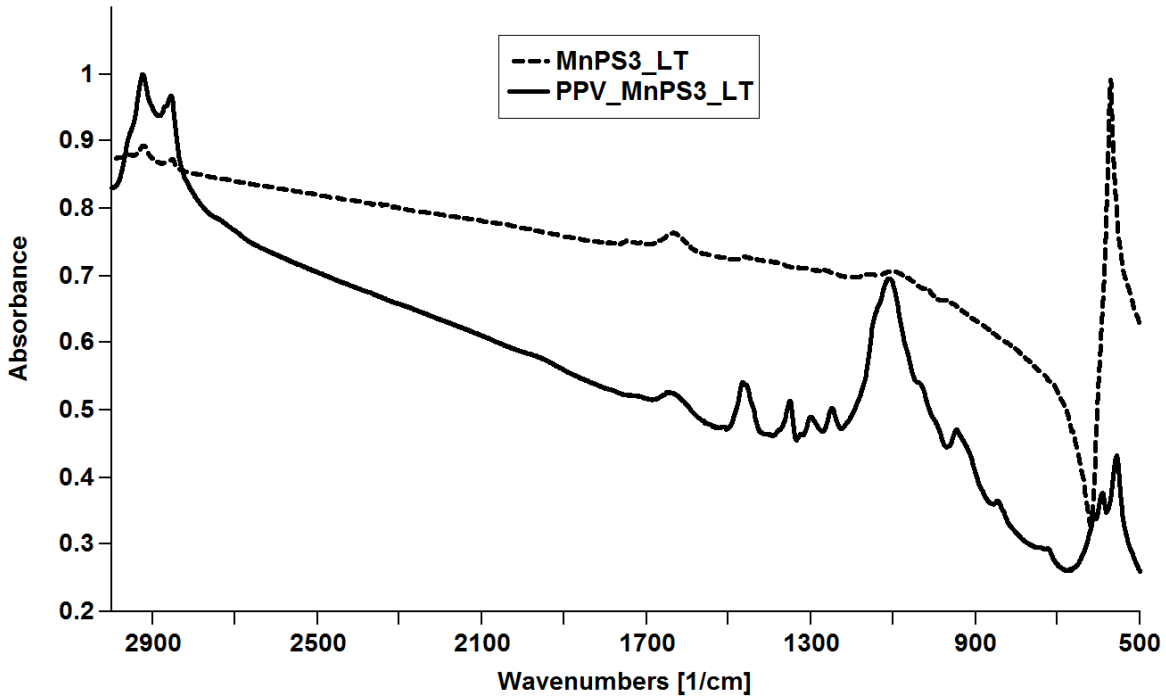

Figure 8: Infrared spectra of $MnPS_3$_LT and PPV-intercalated $MnPS_3$_LT.

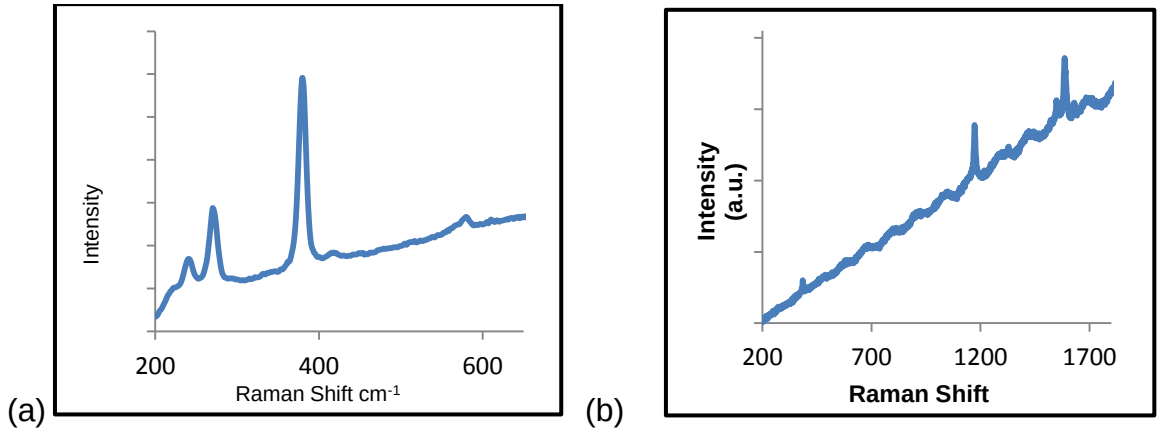

Figure 9: Raman spectra of (a) $MnPS_3$_LT and (b) PPV-intercalated $MnPS_3$_LT.

3.3 Photoluminescence studies

The emission spectra of PPV and PPV-intercalated $MnPS_3$ are illustrated in Figure 10. Both samples were excited at 400 nm. After chemical elimination of the

sulfonium residues, the extent of π–conjugation in the intercalated polymer increased, as shown by a red-shift of the emission with respect to the precursor polymer. Pure PPV emitted green fluorescence with a λ_{max} (0-1 transition) around 547 nm, and other vibronic bands at 515 nm and 587 nm assigned to the 0-0 and 0-2 transitions respectively [27]. The emission spectrum of the intercalated PPV was very similar to that of the pure polymer, except that the intensity of the 0-0 band increased relative to that in pure PPV, whilst the 0-1 was reduced. The emission maximum was blue-shifted (to about 509 nm) relative to that of the un-intercalated polymer. The energy differences between the vibronic bands were approximately 1185 and 1330 cm^{-1} for PPV, and 1330 cm^{-1} for the PPV-intercalated $MnPS_3$ sample. These values are close to significant peaks observed in the Raman spectra, and correspond to the aromatic CC-H and vinylene CC-H bending modes. Our proposed band assignments for intercalated PPV were based on the observed energy differences; however, there is a small unexplained shoulder at 490nm, which may indicate an overlapping process due to the presence of oligomeric species.

Bathochromic (red) or hypsochromic (blue) shifts in emission spectra are usually related to changes in the conjugation length of the polymer chain. In this case, the blue-shift observed for intercalated PPV may indicate that shorter conjugated segments are responsible for the emission process. This could mean that the intercalated polymer inside the inorganic host had conformational defects such as kinks or twists, or more probably, that the elimination reaction forming PPV was incomplete, restricting the π-overlap in the polymer. On the other hand, the changes in shape of the emission envelope are probably due to displacements in the configurational coordinate due to the presence of the inorganic crystal layers. It is known [27-29] that the relative intensities of the vibronic transitions vary with the configurational displacement (ΔQ) of the π and π^* states of conjugated polymers; hence, if ΔQ decreases, the relative intensity of the 0-0 transition increases.[28,29] In this case, the inorganic matrix would be expected to decrease the conformational disorder of the polymer chains confined between the layers [27,28]. If the planarity of the polymer is enhanced, the configurational coordinate displacement (ΔQ) is reduced, and the relative intensity of the 0-0 (509 nm) transition of the intercalated PPV is increased [24,29-30].

The role of the inorganic host matrix was apparently a passive one, since no sensitized PPV luminescence was detected via excitation in the UV region, in which $MnPS_3$ has strong absorptions. On the other hand, the characteristic polymer luminescence showed no sign of weakening over periods of many months in ambient conditions, so the host conferred strong protection against the typical photodegradation of conjugated polymers such as PPV. This protection may not be simply due to the exclusion of atmospheric oxygen from the polymer, and the mechanism will require further investigation.

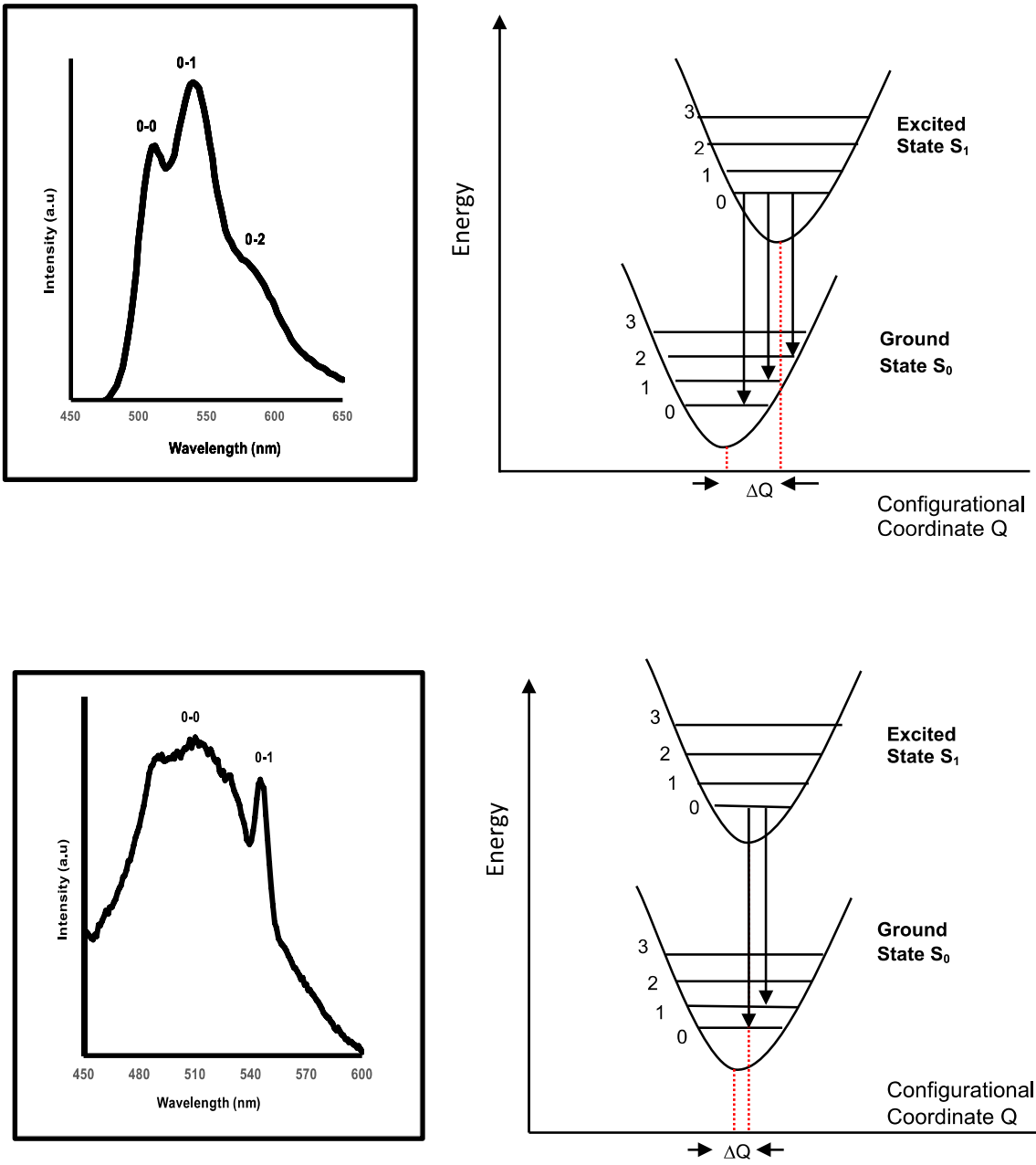

Figure 10: Photoemission spectra of (top) PPV and (bottom) PPV_$MnPS_3$, showing vibronic structure. The corresponding configuration coordinate diagrams are shown on the right.

3.4 Electrical Conductivity

The conductivity of PPV-intercalated high temperature $MnPS_3$ (Table 2) was found to be 25 times that of the pure crystalline host, and five orders of magnitude higher than

that of the un-intercalated polymer. PPV, although a fully conjugated polymer, is an intrinsic electrical insulator, and it requires the use of dopants such as iodine or sodium in order to produce appreciable conductivities [31]. Similarly, $MnPS_3$ is categorized as a wide-gap semiconductor, and it is known to have a high resistivity at ambient temperature [32].

The increased conductivity of the intercalated sample may be attributable to better organization of the polymer chains, which would improve the charge mobility in the organic component of the intercalate. However, there is also the possibility of a small amount of charge-transfer from the comparatively electron-rich guest to the host, making the polymer slightly p-type and the $MnPS_3$ weakly n-type, and enhancing the overall electrical conductivity.

Sample	**Conductivity σ (Sm^{-1})**
PPV	10^{-13} Refs. [26, 30]
$MnPS_3$	2.2×10^{-9}
PPV_$MnPS_3$	5.5×10^{-8}

Table 2: Conductivity of single crystals of $MnPS_3$ and PPV-intercalated $MnPS_3$

The apparent conductivities measured on the uniaxially-pressed powder pellets (Table 3) were much lower than those of the single crystals. It seems likely that the powdered crystal platelets had a preferred alignment parallel to the flat surfaces of the uniaxially-pressed pellets. The measured values would therefore reflect the structural anisotropy of the intercalated materials, and the likelihood that the carrier mobility parallel to the layers is greater than the perpendicular mobility. The phenomenon is less marked for the low temperature-synthesized $MnPS_3$ intercalate, in which the crystallites were much smaller and consequently harder to align.

Sample	**Conductivity σ (Sm^{-1})**
PPV_$MnPS_3$	3.8×10^{-11}
PPV_$MnPS_3$_LT	1.6×10^{-10}

Table 3: Conductivity of pressed pellets of PPV intercalated in crystalline and amorphous $MnPS_3$.

4. Conclusions

This paper has reported work on a well-known luminescent polymer (PPV) intercalated into a stable and convenient lamellar thiophosphate host. For potential applications in light-emitting devices, the stability of such polymers can be improved by entrapment in an inorganic matrix such as clay [7]. Unlike such insulating hosts, $MnPS_3$ was selected here because it is a wide-gap semiconductor with the ability to facilitate electron/hole transport to the polymer, while also being transparent in the spectral region emitted by PPV.

We synthesized $MnPS_3$ by direct elemental combination at high temperature and by a low temperature solution method. Novel nanocomposites with PPV were produced via ion-exchange and subsequent thermal treatment, and were characterized by IR/Raman spectroscopy, X-ray powder diffractometry, thermogravimetric analysis and scanning electron microscopy. The photoluminescence of the hybrid materials showed stable, slightly blue-shifted emission from the PPV. There was a significant increase in the electronic conductivity relative to the pure intercalant and host, which could be advantageous for OLED applications of PPV or similar luminescent polymers.

Acknowledgement

We are grateful to Kingston University for the provision of a Scholarship for IMDM, and to Simon Crust and Richard Giddens for their technical advice and support.

References

1. Eftekhari, A. (2010) *Nanostructured Conductive Polymers*. UK: John Wiley & Sons Ltd.

2. Burroughes, J.H., Bradley, D.D.C., Brown, A.R., Marks, R.N., Mackay, K., Friend, R.H. and Burns, P.L. (1990) Light-emitting Diodes Based on Conjugated Polymers. *Nature*, 347, 6293, 539-541

3. Grindsale, A.C., Chan, K.L., Rainer, E.M., Jokisz, P.G. and Holmes, A.B. (2009) Synthesis of Light Emitting Conjugated Polymers for Applications in Electroluminescent Devices. *Chemical Reviews*, 109, 897-1091.

4. Nazar, L.F., Zhang, Z. and Zinkweg, D. (1992) Insertion of Poly(p-phenylene vinylene) in layered MoO_3. *Journal of the American Chemical Society*, 114, 6239-6240.

5. Cucinotta, F., Carniato, F., Paul, G., Bracco, S., Bisio, C., Calderelli, S. and Marchese, L. (2011) Incorporation of a Semiconductive Polymer into mesoporous SBA-15 Platelets: Towards New Luminescent Hybrid Materials. *Chemistry of Materials,* 23, 2803-2809.

6. Alvaro, M., Corma, A., Ferrer, B., Galletero, M.S., Garcia, H. and Peris, E. (2004) Increasing the Stability of Electroluminescent Phenylenevinylene Polymers by Encapsulation in Nanoporous Inorganic Materials. *Chemistry of Materials*, 16, 2142-2147.

7. Lee, H., Lee, T., Lim, Y.T. and Park, O.O. (2002) Improved Environmental Stability in Poly(p-phenylene vinylene) Layered Silicate Nanocomposite. *Applied Clay Science*, 21, 287-293.

8. Clement, R. (1980) A Novel Route to Intercalation into Layered $MnPS_3$. *Journal of the Chemical Society, Chemical Communications*, 647-648

9. Sukpirom, N., Oriakhi, C.O. and Lerner, M.M. (2000) Preparation of layered nanocomposites of PEO with $MnPS_3$, $CdPS_3$, and MoO_3 by melt intercalation. *Materials Research Bulletin*, 35, 325-331.

10. Foot, P.J.S. and Shaker, N. (1983) Amine intercalates of the lamellar compounds $NiPS_3$ and $CdPS_3$*. Materials Research Bulletin*, 18, 173-180.

11. Coradin, T. and Clement, R. (1998) From Intercalation to Aggregation: Non Linear Optical Properties of Stilbazolium Chromophores-$MnPS_3$ Layered Hybrid Materials. *Chemistry of Materials*, 8, 2153-2158.

12. Oriakhi, C.O. and Lerner, M.M. (2002) Nanocomposites and Intercalation Compounds. *Encyclopedia of Physical Science and Technology*. 3rd edition. USA: Academic Press.

13. Foot, P.J.S. and Nevett, B.A. (1986) *Cathode Material for Alkali-Metal Rechargeable Cell*, United States Patent Office, Patent N^0 4579724; idem., (1987), Properties of $NiPS_3$ and $ZnPS_3$ prepared at ambient temperature. *Journal of the Chemical Society, Chemical Communications*, 380-381.

14. Falius, H. (1968) Hexathiohypophosphate, Salze einer neuen Saure des Phosphors. *Zeitschrift fur anorganische und allgemeine Chemie*, 356, 189-193.

15. Wessling, R.A. and Zimmerman, R.G. (1968) *Polyelectrolytes from Bis Sulfonium Salts,* US Patent 3401152.

16. Li, C., Wang, X., Peng, Q., Li, Y. (2005) Synthesis and Characterization of $Mn_2P_2S_6$ Single-Crystal Nanorods and Nanotubes. *Inorganic Chemistry*, 44 (19), 6641-6645.

17. Yi, T., Clement, R., Haut, C., Catala, L., Gacoin, T., Tancrez, N., Ledoux, I. and Zyss, J. (2005) J-Aggregated Dye-$MnPS_3$ Hybrid Nanoparticles with Giant Quadratic Optical Nonlinearity. *Advanced Materials*, 17 (3), 335-338.

18. Legadic, I., Lacroix, P.G. and Clement, R. (1997) Layered MPS_3 (M=Mn, Cd) Thin Films as Host Matrixes for Nonlinear Optical Material Processing. *Chemistry of Materials*, 9 (9), 2004-2012.

19. Pattayil, A.J. and Vasudevan, S. (1992) The Intercalation Reaction of Pyridine with Manganese Thiophosphate, $MnPS_3$. *Journal of the American Chemical Society*, 114, 7792-7801.

20. Hangyo, M., Nakashima, S. and Mitsuishi, A. (1988) Raman Spectra of $MnPS_3$ Intercalated with Pyridine. *Solid State Communications,* 65 (5), 419-423.

21. Mathey. Y., Clement, R., Sourisseau, C. and Lucazeau, G. (1980) Vibrational Study of Layered MPX_3 Compounds and Some Intercalates with $Co(\eta^5\text{-}C_5H_5)_2^+$ or $C(\eta^6\text{-}C_6H_6)_2^+$. *Inorganic Chemistry*, 19, 2773-2779.

22. Tran, V.H. and Massardier, V. (1996) Spectroscopy Studies of the Conversion of Poly(p-phenylene-vinylene) Precursor. *Polymer*, 37 (11), 2061-2065.

23. Kobryanskii, V.M., Kaplanova, T.G. and Vitukhnovsky, A.G. (1997) Effect of Storage of Precursor Polymer Solution on the Electronic and Physical Structure of Poly(p-phenylene vinylene). *Synthetic Metals*, 84, 257-258.

24. Baitoul, M., Wery, J., Buissons, J.P., Arbuckle, G., Shah, H., Lefrant, S. and Hamdoume, M. (2000) In Situ Resonant Raman and Optical investigations of P-doped Poly(p-phenylene). *Polymer*, 41, 6955-6964.

25. Aarab, H., Baitoul, M., Wery, J., Almairac, R., Lefrant, S., Faulques, E., Duvail, J.L. and Hamedoun, M. (2005) Electrical and Optical properties of PPV and Single-walled Nanotubes Composites Films. *Synthetic Metals*, 1, 63-67.

26. Webster, S. and Batchelder, D.N. (1996) Absorption, Luminescence and Raman Spectroscopy of Poly(p-phenylene vinylene) at High Pressure. *Polymer*, 37 (22), 4961-4968.

27. Yoon, K.H., Park, S.B. and Yang, B.D. (2004) Size Effect of Nanoparticles on the Conjugated Polymer in PPV/SiO_2 Nanocomposites. *Materials Chemistry and Physics*, 87, 39-43.

28. Zhang, J., Wang, B., Ju, X., Liu, T. and Hu, T. (2001) New Observations on the Optical Properties of PPV/TiO_2 Nanocomposites. *Polymer*, 42, 3697-3702.

29. Skotheim, T.A., Elsenbaumer, R.L. and Reynolds, J.R. (1998) *Handbook of conducting polymers*. 2nd edition. USA: Marcel Dekker, Inc.

30. Bakueva, L., Matheson, D., Musikhin, S. and Sargent, E.H. (2002) Luminescence of Pure and Iodine Doped PPV: Internal Energetic Structure Revealed through Spectral Signatures. *Synthetic Metals*, 126, 207-211.

31. Mishra, U.K. and Singh, J. (2008) *Semiconductor Device Physics and Design.* Netherlands: Springer.

32. Grasso, V., Neri, F., Santangelo, S., Silipigni, L. and Piacentini, M. (1989) Electronic Conduction in the Layered Semiconductor $MnPS_3$. *Journal of Physics: Condensed Matter*, 1, 3337-3347.